Check for updates

Nonthermal Plasma Treatment for Electrocatalysts Structural and Surface Engineering

Jiayi Tang, Chao Su, and Zongping Shao*

Structure and surface modification of electrocatalysts demonstrates a promising lead for achieving excellent electrocatalytic activity and efficiency. Among various surface modification strategies, nonthermal plasma technique possesses an irreplaceable role due to the merits of simple but controllable operation procedure, low pollution, low cost, and easy scale-up for practical applications. Nonthermal plasma treatment, as a powerful tool for material surface and structural engineering, can mainly benefit the electrocatalytic reactions in the following aspects: surface atom doping or reconstructing, introducing vacancies or defects, surface partially reducing or oxidizing, and increasing the porosity or roughness. Given to its flexibility, plasma modification is gaining a noticeable popularity, and great progress has been made in applying plasma for optimizing surface properties of the mainstream electrocatalysts, including metal-free carbon materials, metal oxides, and other compounds, as well as organometallic electrocatalysts, etc. This review first summarizes the recent advances in nonthermal plasma modification for achieving desirable electrocatalytic behaviors, aiming to highlight the cutting-edge function designs of electrocatalysts with plasma technology. It is hoped that this work can give some inspiration for the development of highly efficient electrocatalysts.

J. Tang, Z. Shao
WA School of Mines: Minerals
Energy and Chemical Engineering
Curtin University
Perth, WA 6102, Australia
E-mail: zongping.shao@curtin.edu.au

C. Su
School of Energy and Power Engineering
Jiangsu University of Science and Technology
Zhenjiang 212003, China

Z. Shao
State Key Laboratory of Materials-Oriented Chemical Engineering
College of Chemical Engineering
Nanjing Tech University
Nanjing 211816, China

The ORCID identification number(s) for the author(s) of this article can be found under https://doi.org/10.1002/ente.202200235.

1. Introduction

It has been well recognized that the performance of electrocatalysts is governed by the surface properties. Plasma is essentially an ionized substance, which could be generated when sufficient energy is imposed to a certain gas medium or a gas mixture. The energy sources are extensive for generating plasma, including flames, combustion, heats, electric discharges (plasma jets, spark, arc, glow, corona, radio frequency [RF], and microwave), and dielectric barrier discharge (DBD), as well as shocks driven by electricity, magneticity, chemical reactions, etc. As early as the 1990s, plasma technology was favored by researchers as an alternative way for the preparation of catalysts.[1] In addition to direct synthesis, plasma technology has gained noticeable popularity in the modification of the electrocatalysts surface, which is also known as plasma-enhanced preparation strategies.[2] According to the 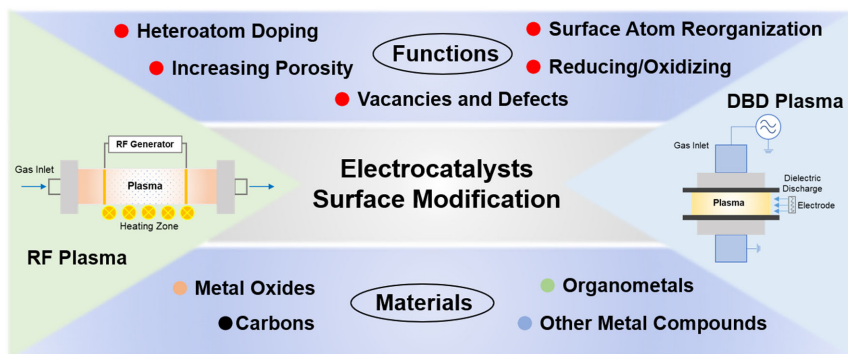energy level, the generated plasma can be classified as high-temperature plasma and low-temperature plasma. The plasma used for catalyst preparation and treatment in laboratory and industry usually belongs to the low-temperature plasma.[3] In low-temperature plasmas, those used for catalyst surface modification usually refer to the nonthermal plasma, which is also called cold plasma or nonequilibrium plasma. The highly energetic ions in plasma possess higher chemical activity than those in the diffusion-limited thermal reactions,[4] thus making plasma surface treatment a powerful tool for electrocatalysts modification. Among various nonthermal plasma techniques, RF-generated plasma and DBD-generated plasma are most commonly used for electrocatalysts modification, as shown in **Figure 1**. RF-generated plasma is featured with low gas temperature, but high electron temperature (typically 10^4–10^5 K), while DBD-generated plasma by using dielectric barrier can restrain the instability during discharge to keep a low gas temperature. The main difference between the electric discharge and dielectric discharge was believed to be the shape of the applied electric field. The electric field created by barrier discharges could be relatively homogeneous in the whole gap. While in barrier discharges, the electron density is higher than that in a typical electric discharge, but the electron is featured with a lower temperature.[5]

Under the excitation impact by external energy, the fast electrons act on different gas molecules; thus, the reactive species,

**ADVANCED
SCIENCE NEWS**

www.advancedsciencenews.com

Energy Technology
Generation, Conversion, Storage, Distribution

www.entechnol.de

Figure 1. Schematic illustration of plasma techniques used for material surface modification to realize functionalization of the electrocatalysts.

such as excited atomic O, N, S, and P radicals, as well as molecular O_2^+, N_2^+, H_2^+, NH_2^-, and OH^- radicals, can be generated under certain atmosphere composition and operating conditions. The interactions between the electrocatalyst surface and plasma-generated radicals can bring various functions to the catalyst, such as reorganizing surface atoms,[6] introducing vacancies and/or defects,[7] doping with heteroatoms,[8] partially reducing or oxidizing surface,[9] as well as enhancing the roughness and/or creating porosities,[10] to favor the electrocatalysis activity of the material. Traditional chemical synthesis/modification strategies, involving the ionic surfactants and wet chemical covalent functionalization process, are usually accompanied by harsh operating conditions, and the chemical reagents used can cause detrimental effects to the environment.[11] In contrast, unnecessary thermalization during the plasma treatment is usually expected to be circumvented. The unique advantage of plasma modification is that this technique enables the controllable modification of the electrocatalyst surface properties, while produces minor effect on the bulk structure of the material, thus to realize highly distributed active sites on various carriers.[12] Moreover, impressive as its operating simplicity, short preparation time, plasma technology was soon promoted as a key approach to engineer nanostructured catalysts.

This review deliberately summarizes the research progress made in using nonthermal plasma treatments for electrocatalyst surface modification from the perspective of the mechanism behind this technique. The operating parameters in plasma treatments have been specified to provide instructions on potentially use of this tool for electrocatalysts surface functionalization. Recent advances in plasma surface modification for achieving desirable electrocatalytic performance of carbons, metal oxides, and other compounds, as well as organometals, have been thoroughly reviewed and analyzed. To some extent, we hope this work can provide impetus to explore nonthermal plasma treatment as a feasible way for electrocatalysts modification.

2. Mechanisms for Plasma-Induced Material Surface Modification

Plasma-generated excited species can interact with the first few atomic layers on the material thus results in physical and/or chemical modification of the material surface, while maintaining

the properties of the bulk. Plasma treatment mainly tunes the surface properties of the material by the following ways: 1) The excited radical species can react with materials surface to form new chemical bonds, resulting in new doping functionalities. 2) The high energy radicals in plasma could attack the material surface to subsequently exfoliating or engraving the material surface to increase roughness and porosity. 3) The redox ions generated in plasma can partially reduce or oxide the material surface to tune the electronic properties of the active sites.

2.1. Chemical Modification to Dope Functionalities

Impact ionization is the main mechanism to explain the generation of plasma. In a local electric field impacted by certain energy, electrons are accelerated and then to ionize background gas atoms or molecules to create more electrons and reactive species, which can chemically modify the material surface.[13] For example, in air, this impact ionization mainly takes place via the following reactions

$$N_2 + e \rightarrow N_2^+ + 2e \tag{1}$$

$$O_2 + e \rightarrow O_2^+ + 2e \tag{2}$$

Meanwhile, the excited N and O radicals can further react with the gas molecules to form nitrogen–oxygen compounds through the following reactions[14]

$$N + O_2 \rightarrow NO + O \tag{3}$$

$$O + N_2 \rightarrow NO + N \tag{4}$$

With the existence of water in air, the OH radical can also be created[15]

$$H_2O + e \rightarrow H + OH + e \tag{5}$$

Note that the above equations mainly cover the ways of electron-induced dissociation for radical generation; other side reactions within reactive species and dissociative electron recombination processes could be more complicated.[16] After all, it is certain that the reactive species generated in discharge is dominated by the electron energy, which can be controlled by tuning the power as well as the gas composition.[17] For example, the O_2^+ radical generated in oxygen plasma can break the C—C, C—H,

and C—N bonds on the carbon fiber surface to form C radicals. The excited O radical may further react with the O_2 molecules to generate more reactive oxygen species (like O^+, O^{2+}, O_2^+, and O_2^{2+}). These O reactive species then react with the C radicals to form various oxygen functional groups, such as —OH, —COOH, and —C≡O, thus realize chemically modification of the material surface.[18] Hydrogen plasma with the generated active species, such as H^+, H_2^+, and H_3^+, could deliver much higher oxygen-absorbing capability than molecular hydrogen, thus can effectively reduce the oxides surface in mild conditions.[19] Nitrogen plasma conducted with N_2 or NH_3 is likely to generate N^+, N_2^+, or NH_2^-, which are capable of incorporating N-atoms to the graphitic lattice.[20] While in the case of NH_3 plasma, the generated H-containing NH_2^- species may provide additional reducing effect to the oxide surface.[21] Similar cases have been reported by using sulfur plasma and phosphorus plasma treatment to achieve S-doping and *P*-doping to materials, but the hazard to environment is unlikely to be circumvented in these cases by using H_2S or PH_3 gaseous precursors.[22]

2.2. Physical Modification to Increase Surface Roughness

Engineering of carbon electrocatalysts with more edges/defects has been demonstrated to be a novel strategy to enhance the catalytic performance.[23] Ar plasma has shown physical etching effect, which can be used to generate pores and rich edges/defects on carbon materials, such as carbon nanotubes, graphite, and graphene as efficient metal-free electrocatalysts. For example, Tao et al. reported the use of Ar plasma with optimized operating time and temperature for the synthesis of dopant-free graphene catalyst for the oxygen reduction reaction (ORR).[7c] Physical characterization indicated that the plasma etching increased the active edge sites on the carbon surface, while maintained the bulk integrity of the edge-rich graphene without causing damage to the macroscopic structure. Without any other dopants, the results confirmed the critical role of edge-rich surface of carbon catalysts with higher charge densities for benefiting the electrocatalytic ORR performance.

Given to the simplicity and flexibility of the operation process of plasma treatment, it has been used for rapid in situ exfoliating/engraving of the substrate to expose more active sites. For example, Liu et al. demonstrated the direct generation of active sites on carbon cloth by treating with Ar plasma to serve as bifunctional electrocatalyst for the ORR/oxygen evolution reaction (OER).[24] The synthesis procedure is illustrated in **Figure 2**A; the as-exfoliated graphene by plasma treatment with large amount of pore structure and edges/defects-rich surface was then reacted with oxygen when exposed to air. As a result, the graphene surface functionalized by oxygen groups was formed and exhibited better electrolyte affinity with much enhanced mass transport to the active sites. Figure 2B presents a simulated process of charge transfer on defective graphene functionalized by electronegative oxygen groups; the introduced functional oxygen groups can withdraw electrons from adjacent carbon atoms, resulting in more positively charged carbon atoms, which also facilitated the adsorption of intermediate reaction species during the electrocatalysis ORR and OER process.[25]

Similarly, $Co(OH)_2$ nanosheet arrays were reported to be directly electrodeposited on nickel foam accompanied by air
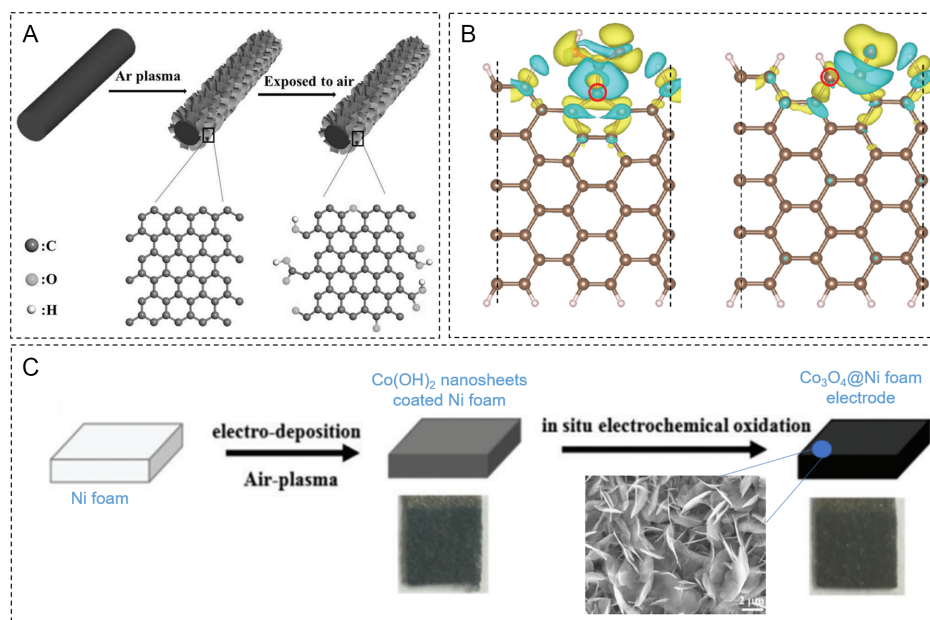
Figure 2. A) Schematic illustration of the in situ synthesis of defective and oxygen-functionalized graphene from carbon fiber. B) Illustration of charge transfer on defective graphene surface with C—OOH species (left) and nondefective graphene with C≡O species (right). Yellow and blue indicate negative and positive charge, respectively; brown, white, and yellow balls represent carbon, hydrogen, and oxygen atoms, respectively; red circles mark the most active sites. Adapted with permission.[24] Copyright 2017, WILEY-VCH. C) Scheme of in situ fabrication of Co_3O_4@Ni foam porous electrode engraving by air plasma with insert scanning electron microscopy (SEM) image of the as-formed porous electrode. Adapted with permission.[26] Copyright 2017, The Royal Society of Chemistry.

plasma to engrave more active defects (Figure 2C).[26] The as-formed $Co(OH)_2$ nanosheets after in situ oxidation were converted to Co_3O_4 oxide electrode with distinct porous architecture, as shown in the insert SEM image in Figure 2C. The favorable OER kinetics could be attributed to the morphological features with abundant active sites and large specific surface area of the electrode, as well as the fast gas release from the rough electrode surface to reduce the ohmic loss at the interface between the catalyst and electrolyte.

2.3. Partially Oxidizing/Reducing Surface

Tuning the oxidized state of metal active sites has been proposed to be an effective way for enhancing the electrocatalytic performance.[27] One typical case is the oxidized copper (Cu) catalyst developed for the carbon dioxide reduction (CO_2RR),[28] where the existence of Cu^+ species was suggested to play a critical role in reducing the onset potential and enhancing product selectivity.[9,29] O_2 plasma and H_2 plasma were used synergistically to tune the chemical state on the polycrystalline Cu.[9] Cross sections of the plasma-treated Cu foils were measured using scanning transmission electron microscopy (STEM) combined with elemental mapping using energy dispersive spectrometer (EDS), as shown in **Figure 3**A–D; O_2 plasma treatment under 20 W for 2 min resulted in a well-defined thicker Cu_2O interlayer with a thinner CuO top layer. The afterward H_2 plasma treatment reduced the surface to form an apparent 100 nm-layer metallic Cu, with the CuO and Cu_2O oxide remaining in the subsurface. The as-formed nanostructured Cu oxide layers remained during electrocatalysis reaction provided direct evidence to the key role of the oxidized Cu^+ as the active sites for CO_2RR.

Sometimes, surface modification on transition metal oxides by partially reducing the surface atoms is considered to be effective for enhancing the electrical conductivity of this kind of materials for electrocatalysis.[31] Carbon plasma was applied to produce reduced Ni_4Mo component on $NiMoO_4$ nanowire arrays.[30] A short treatment process of 30 s was conducted and demonstrated to result in the exposure of more active Ni–Mo sites on the surface by forming Ni_4Mo nanoparticles (Figure 3E), while maintained the nanowire array structure of the electrocatalyst. In addition, a thin layer of carbon shell was deposited on the nanowire surface, which may effectively prevent the loss of active sites during electrocatalysis reaction, and render the catalyst with higher chemical stability. The surface chemical composition and valence states changes, as exhibited by X-Ray photoelectron spectroscopy (XPS) characterizations of Ni $2p_{3/2}$, Mo $3d$, and O $1s$ spectra in Figure 3F-H, were indexing to the formation of metallic Ni and Mo in lower valence state, and decreased O^{2-} ions in crystal structure after plasma treatment.

3. Operating Parameters in Plasma Treatments

Plasma-induced material surface modification can be adjusted by precise control of the processing parameters, such as gas composition, partial pressure, plasma generator power, exposure time, etc.[32] The changes taken place with the surface functionalities are likely to be the substantial effect on the electrocatalytic performance of plasma-treated electrocatalyst. Sometimes the critical values of different operating parameters on the final modification effects are synergistic. Herein, we select some representative examples for investigating the influence of single factor or coupling factors on material modification for brief discussion.
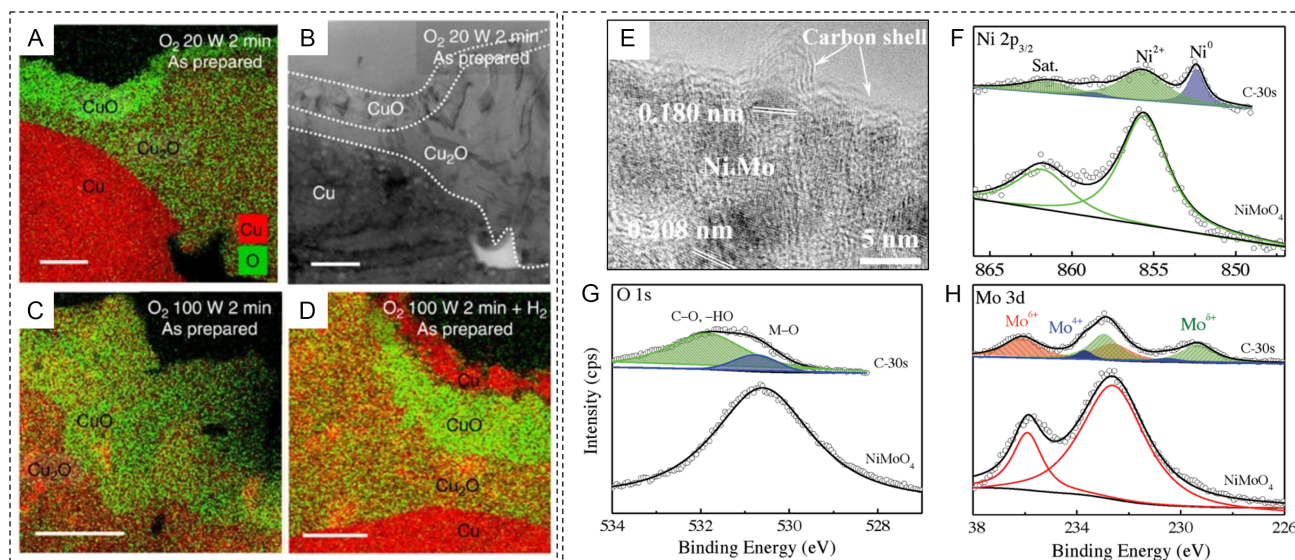
Figure 3. Morphological characterization of the plasma-treated Cu foils: A) EDS elemental mapping, and B) STEM image after O_2 plasma treatment under 20 W for 2 min; C) EDS elemental mapping after O_2 plasma treatment under 100 W for 2 min, and D) subsequent H_2 plasma treatment. Reproduced under the terms of the Creative Commons CC-BY License.[9] Copyright 2016, The Authors, published by nature Publishing Group. E) High resolution transmission electron microscopy image of the carbon plasma-treated $NiMoO_4$ nanowire arrays with reduced Ni_4Mo alloy nanoparticles and thin carbon shell; XPS characterizations of F) Ni $2p_{3/2}$, G) O $1s$, and H) Mo $3d$, confirming the changes of chemical composition and valence states of the sample after plasma treatment. Adapted with permission.[30] Copyright 2018, WILEY-VCH.

**ADVANCED
SCIENCE NEWS**
www.advancedsciencenews.com

Energy Technology
Generation, Conversion, Storage, Distribution
www.entechnol.de

3.1. Gas Composition

Plasma treatments conducted under different gaseous or liquid feedstocks, typically H_2, O_2, Ar, N_2, H_2O, CH_4, ethanol, H_2S, PH_3, etc., have been commonly used to modify the material surface through chemical reactions between the excited free radicals and material surface.[17,33] Zhang et al. recently reported the incorporation of H into α-Ti crystal lattice by H_2 plasma bombardment. The H-activated Ti plate was featured with a partially reduced surface oxide layer, and exhibited improved performance toward electrocatalytic HER.[19a] Besides introducing heteroatom doping or functional groups to the material surface, investigation toward tuning the feedstock composition in plasma treatment has found possibilities in achieving desirable surface reorganization for electrocatalysis. For example, Ar/O_2 plasma was reported to controllably introduce oxygen doping to modify $FePSe_3$ nanosheets, meanwhile bring surface reorganization by forming an amorphous phase on crystalline interface. Another example by employing plasma with two different gases has been reported to enhance the ORR performance of carbon nanotubes without heteroatom doping.[34] Mild plasma irradiation with Ar and NH_3 atmosphere was suggested to introducing more topological defects to the nanotubes, as well as bringing a healing effect to the sp^3 bonds. In this case, it was found that not the nitrogen dopant, but the Stone–Wales defects and vacancies generated by plasma treatment under two gases are more likely to contribute to the enhanced catalytic activity toward the ORR.[35]
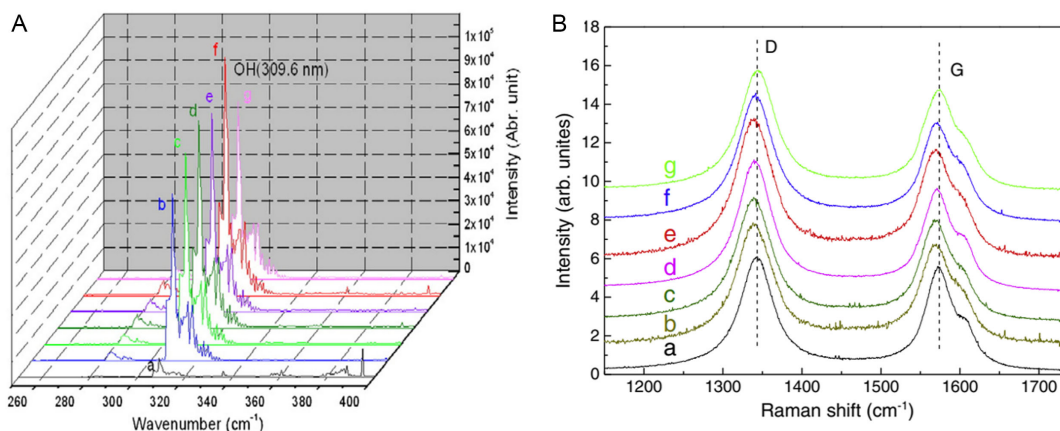
3.2. Partial Pressure

The pressure or partial pressure of gas feedstock in plasma processing can strongly affect the modification. The gas pressure, which is positively correlated to the electron density, mainly affects the oscillation in plasma treatment.[36] Khaledian et al. studied the operating pressure in Ar plasma for the treatment of rutile phase TiO_2.[37] It was found that the decrease of pressure can subsequently enhance the velocity of Ar particles and the electrical field, resulting in more collision of the electrons with

higher power to the TiO_2 surface. Chen et al. studied the emission spectra of Ar/H_2O plasma with different Ar partial pressure by optical emission spectroscopy (OES).[38] As shown in **Figure 4**A, the 309.6 nm line represents the OH radicals generated by the de-excitation of H_2O molecules. The active OH radical is highly reactive with the surface atoms of multiwall carbon nanotube (MWCNT), thus mainly attributes to the formation of surface bindings with oxygen-containing groups. Increase the fraction of Ar was able to first increase the content of OH radical in plasma and then reduce it to a certain extent. Raman spectra, as shown in Figure 4B, were conducted to further confirm the modification effects with varied Ar pressure. The I_D/I_G ratio, which is corresponding to the structural defects with the incorporation of oxygen atoms, exhibited a trend of increasing first and then decreasing. Therefore, the gas pressure should be well controlled to avoid damage to the material surface during plasma modification.

3.3. Process Time and Generator Power

The treatment time and generator power in plasma modification should be a pair of coupling factors. Generally, it is recognized that shorter time is required with higher power plasma generator for reaching a plateau state of surface modification.[32] Oxygen plasma for the treatment of nanotubes has been studied with varied generator power from 20 to 60 W, and process time from 0.1 to 30 min.[39] As illustrated in **Figure 5**A, the critical effects of generator power and treating time for oxygen functional groups incorporation and amorphization were identified. The increased work function of plasma gave rise to the surface oxygen groups as indicated by the magenta shadowing, while the surface amorphization indicated by the grey shadowing was identified with the work function decrease. Raman spectroscopy (Figure 5B) as a function of process time exhibited a significant decrease in the intensity of the G band, which was attributed to the formation of amorphous carbon layer on the surface of MWCNTs. The results demonstrate the possibility to confine the material surface

Figure 4. A) OES spectra of Ar/H_2O mixture gas plasma with varied gas partial pressure: a) 13.3/0 Pa, b) 0/13.3 Pa, c) 3.3/10.0 Pa, d) 6.65/6.65 Pa, e) 10.0/3.3 Pa, f) 12.0/1.3 Pa at a generator power of 700 W, and g) 10.0/3.3 Pa at 400 W. B) Raman spectra of a) pristine MWCNTs, and Ar/H_2O plasma-treated samples at varied gas partial pressure: b) 0/13.3 Pa, c) 3.3/10.0 Pa, d) 6.65/6.65 Pa, e) 10.0/3.3 Pa, f) 12.0/1.3 Pa, and g) 13.3/0 Pa. Adapted with permission.[38] Copyright 2010, Elsevier B.V.
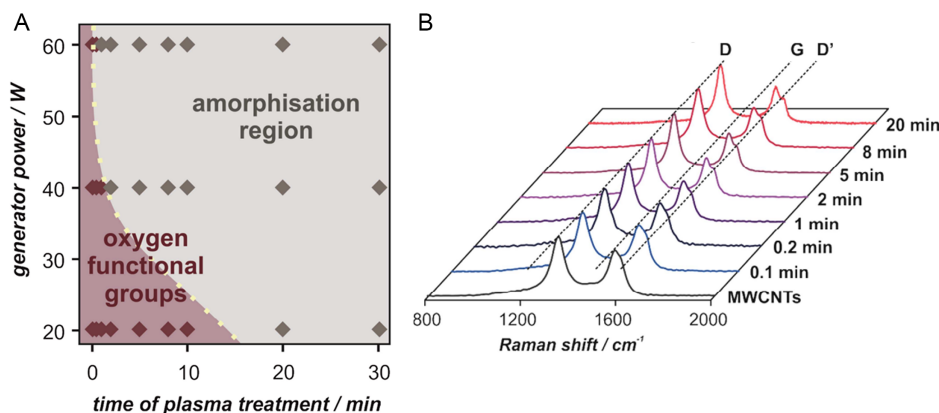
Figure 5. A) Illustration of the modification effects on MWCNTs by plasma treatment at varied generator power and process time. B) Raman spectra of the plasma-treated MWCNTs as a function of process time. Adapted with permission.[39] Copyright 2018, Elsevier Ltd.

modification while preventing degradation of the structure by precise controlling the treatment power and time.

4. Modification of Metal-Free Carbon Electrocatalysts by Plasma Treatment

Heteroatom (typically N, O, B, S, P, F, etc.)-doped carbons, by implanting alien atoms into the sp^2 carbon lattice or introducing heteroatom functional groups onto the carbon edge sites or basal plane by covalent bonds, have been demonstrated to show high promise for electrocatalysis reactions.[40] Heteroatom doping should be a critical feature brought by the plasma treatment of carbon materials under different gaseous environment. Besides, accompanied by the collision of the energetic radicals, defects are generally created on carbon surface during plasma treatment. Metal-free heteroatom-doped carbon-based catalysts have been mainly recognized as promising candidates for the ORR. From one aspect, introducing electronegative atoms (like N) would generate a positive charge density on the adjacent carbon atoms, which could facilitate the oxygen adsorption and charge transfer process.[41] Besides, the specific modification by doping with less electronegative atoms such as B and P was believed to facilitate the reducing process of the adsorbed oxygen molecule.[42]

4.1. N-Doped Carbons

NH_3, N_2, and mixture of $N_2/H_2/NO_x$ plasmas have been used to introduce N-containing functionalities (including pyridinic N, pyrrolic N, quaternaric N, and graphitic N) to the carbonaceous materials, which can serve as the active sites for electrocatalysis reactions.[43] Subramanian et al. first reported the preparation of N-doped vertically aligned carbon nanotubes (VA-CNTs) by nitrogen plasma and studied the electrocatalytic activity for ORR in alkaline solution.[44] After nitrogen plasma treatment, the VA-CNTs presented pyrrolic and quaternary N-functional groups at the surface. Besides, upon exposure to air, oxygen functional groups were also found to be introduced onto the surface along with the N-functional groups. The plasma-treated electrochemical interface was found to be able to reduce oxygen at a lower

overpotential, whereas the mechanism was not clear. To decouple the chemical doping effects and the structural changes in influencing the electrocatalytic performance of carbon, Hoque et al. recently investigated the plasma process to introduce N-sites and isolated C-defects to amorphous carbon thin films.[45] It was found that plasma treatment can be used to simultaneously modify the disordered carbon surface with functional sites, and increase the amorphization degree. From plasma exposure, a mixture of N-functional groups, including pyridinic-N, pyrrolic-N, graphitic-center, graphitic-valley, and N-oxides, was introduced to the carbon surface. Increasing the exposure time showed less contribution to the N-doping effects, while resulted in higher amorphization of the carbon scaffold, as reflected by the Raman spectra in **Figure 6**A. Balancing of the N-doping and structural disorder in plasma treatment could be essential for modulating the electrocatalytic performance toward the ORR process. The sample with 5 min plasma treatment (termed as anC:Np5), though have similar surface N/C concentration with 20 min treated counterpart (anC:Np20), exhibited lower onset potential (Figure 6B), as well as lower yields of hydroperoxide (Figure 6C).

In recent years, plasma has been used for the pretreatment of carbon-based supports to promote the electrocatalytic activity. Pretreated carbon support by plasma was reported to enable a high surface concentration of metal active sites.[46] For example, plasma-activated carbon surface with N-doping functional groups was proposed to assist the chelating of the metal sites and nitrogen centers on the carbon matrix to stabilize the active sites during the following synthesis procedures. NH_3 plasma-generated H-containing species to some extent may protect the carbon support from being oxidized.

4.2. O-Containing Groups Modified Carbons

Oxygen plasma irradiation was used to induce CNT with oxygen-containing groups and tune the charge distribution around the doped heteroatom to promote the ORR.[47] By using a mixture of O_2/H_2O as the feedstock, the excited decomposition of H_2O would generate hydroxyl radicals (OH), and the surface carbon atoms mainly undergo the following chemical reactions with
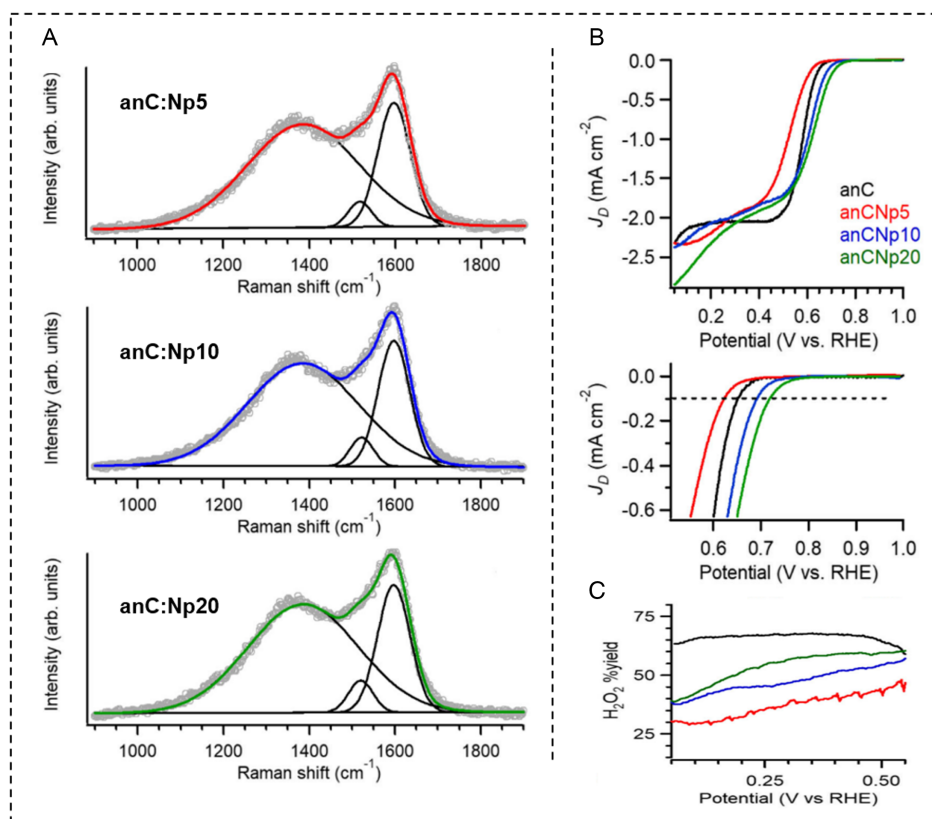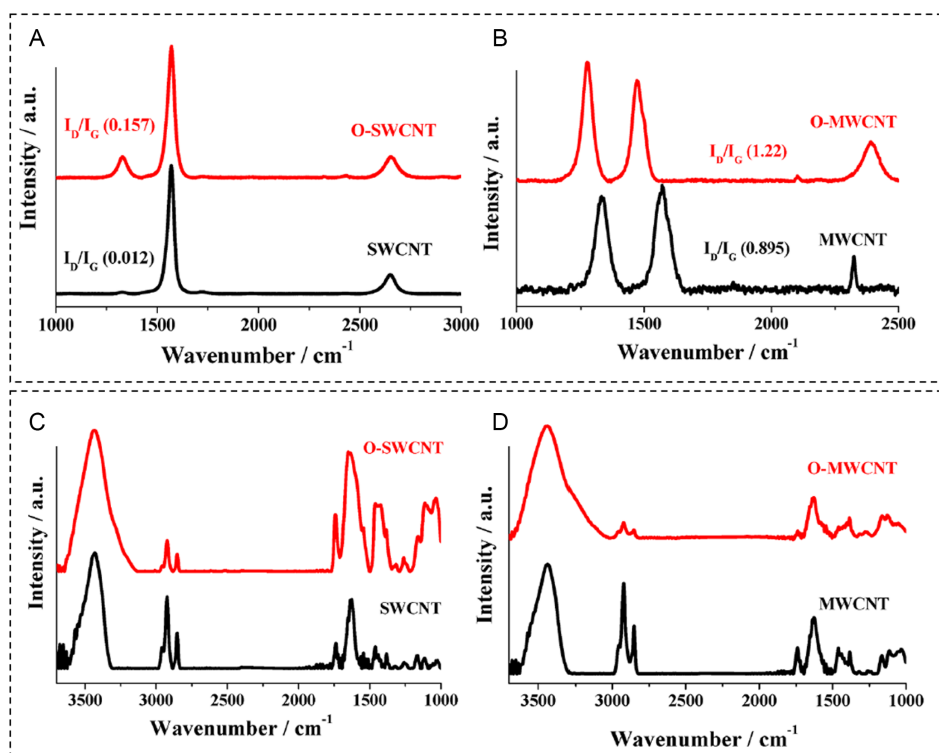
Figure 6. A) Raman spectra and corresponding peak-fits of amorphous carbon thin films: anC:Np5, anC:Np10, and anC:Np20 with plasma treatment for 5, 10, and 20 min, respectively. B) Liner sweep voltammetry obtained under rotating-disk-electrode system in O_2-saturated 0.1 M KOH solutions at 50 mV s^{-1} and 900 rpm. C) The calculated yields of hydroperoxide as a function of potential. Adapted with permission.[45] Copyright 2020, Frontiers.

attack of the active species: hydroxyl bonds are stabilized and formed from exposure to water containing air atmosphere with plasma treatment or from the hydrogen atom transfer from the adjacent reactive carbon atoms, and carbonyl bonds are resulted from an intramolecular reorganization of C—C bonds; while the carboxylic groups are originated from the previously generated active carbonyl bonds and then stabilized by proton transfer, or from the oxidation of C—OH bonds at the terminal carbon. Raman spectral measurements of plasma-treated CNTs, as shown in **Figure 7**A,B, demonstrated the increased ratio of the disorder in the graphene structure compared with pristine CNTs, through the observable increased ratio of the D band intensity to the G band intensity (I_D/I_G), corresponding to the increased sp^3 content in the sp^2 nanotubes. Confirmed by Fourier transform infrared spectroscopy (FT-IR) analysis (Figure 7C,D), the plasma-treated CNTs showed decreased C=C stretching (at 1630 cm^{-1}) and increased C=O stretching in —COOH and C—C=O (at 1753 and 1740 cm^{-1}, respectively), which can be attributed to the forming of oxidized sp^3 edge with the cleavage of the C=C bond. Pristine SWCNT and all the oxygen-plasma treated samples (O-SWCNT) showed $2 + 2e^-$ ORR pathway, while the calculated electron transfer of the counterparts O-MWCNT samples varies from 3.1 to 3.6, close to a $4e^-$ pathway. The induced oxygen sites by plasma treatment were proposed to facilitate the reduction of O_2 to yield hydrogen

peroxide ions (HO_2^-) first and then promote the further reduction of HO_2^- to OH^- in alkaline electrolyte.

The origin of the ORR activity on CNTs is controversial. Waki et al. indicated that the ORR activity could come from the formation of high edges and hole defects.[48] As after the removal of surface oxygen functionalities by annealing process in Ar atmosphere at 900 °C, a positively shifted onset potential of ≈0.73 V versus RHE was achieved, indicating an improvement of ORR activity. However, the oxygen functionalities were also reported to play critical role in electrocatalysis, though do not directly partake the reaction. The enhanced ORR activity could also be attributed to the newly created active sites through the reconstruction of the C defects occurring by the removal of CO desorbing functional groups during the annealing process, while the structural integrity and conductivity of CNTs were maintained. Zhang et al. studied the role of oxygen functional groups within nitrogen-doped carbons for electrocatalytic ORR performance.[49] It was proposed that the existence of quinone-type oxygen groups is the main contributor, in corporation with pyridinic-N active centers to enhance the ORR activity.

Plasma is also applied to carbonaceous materials to increase the surface hydrophilicity, which is preferable for achieving uniform and stable self-dispersion without the aid of dispersing agents. At early stage, introducing hydroxyl and/or carboxyl groups through

**ADVANCED
SCIENCE NEWS**

www.advancedsciencenews.com

Energy Technology
Generation, Conversion, Storage, Distribution

www.entechnol.de

Figure 7. Raman spectra of A) SWCNT, and B) MWCNT before and after oxygen plasma treatment; FT-IR spectra of C) SWCNT, and D) MWCNT before and after 20 min oxygen plasma exposure. Adapted with permission.[47] Copyright 2019, American Chemical Society.

chemical modification was demonstrated to increase the hydrophilicity of the carbon surface.[50] Ar/H_2O plasma has also been used to tune the surface hydrophilicity to improve the dispersion of CNTs.[38] It was found that well-dispersed state of Ar/H_2O plasma-treated MWCNTs could be maintained after 20 days of settling, while varying degrees of agglomeration were observed with the untreated and the Ar plasma-treated counterparts. The oxygen-containing groups that introduced onto the surface of MWCNTs by plasma treatment were considered to be the main factor making the surface hydrophilic.

4.3. Other Heteroatom (i.e., B, S, and F)-Doped Carbons

Introducing different heteroatoms to carbon substrates can be realized by plasma modification. For example, in boron (B)-doped carbon nanotubes, the lower electronegativity of B atom with the vacant $2p^2$ orbital decides that it can extract electrons when conjugated in the carbon π system to form electropositive B sites.[51] Similarly, in fluorine (F)-doped carbons, due to the strong electron affinity of F atoms, charges of the carbon framework could be able to delocalize.[52] In these cases, the adsorption and dissociation behaviors of O_2 molecules may be facilitated to favor the ORR activity. Chokradjaroen et al. reported the dual doping of B and F atoms to carbon by one-step plasma modification with the existence of organic fluorophenyl-boroxin molecules.[53] The enhanced electrocatalytic ORR performance on B-doped carbon was attributed to the electropositive defect sites of the doping B atoms (**Figure 8**A), while the dual doping
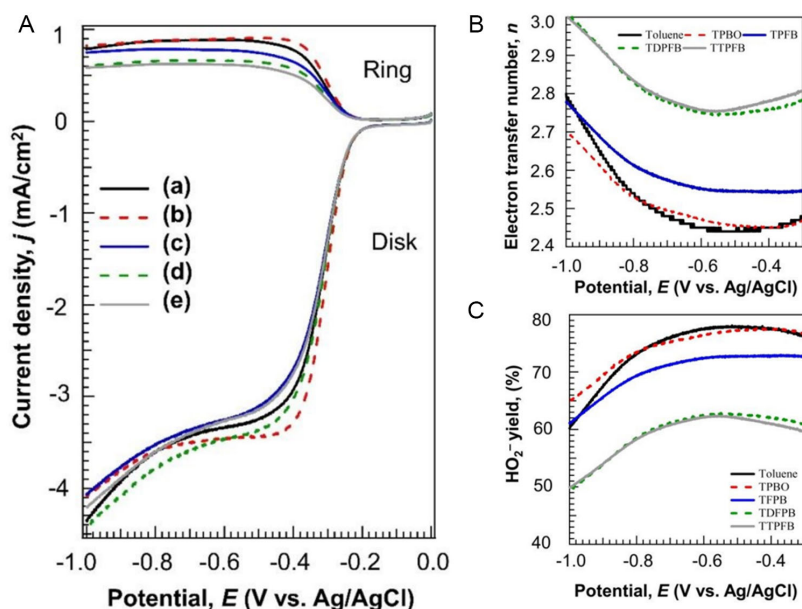
of B and F atoms though did not significantly change the electro-catalytic activity toward ORR, they did show higher values of electron transfer (Figure 8B) and lowered generation of HO^{2-} (Figure 8C) during the ORR process, which suggested a favorable four-electron pathway of ORR as a result of the dual-doping effects.

The synthesis of sulfur (S)-doped carbon recently has been reported by Li et al. and potentially used as support material for Pt nanoparticles with stronger affinity. The plasma reaction under thioanisole (C_7H_8S) goes through the formation of carbon nanoparticles with the breakage of C—S bond, and the excited ·C_2 and ·CH species are generated to assist the growth of long carbon chains to form S-doped carbon nanoparticles. The S-doped carbon support was able to sustain the mass activity of Pt nanoparticles during electrochemical reaction cycles.[54] H_2S plasma treatment was used to simultaneously exfoliate and thermally reduce the graphene surface.[22e] The results showed that S plasma modification of different graphite oxides generally brought positive correlation to the catalytic activity of graphene materials toward ORR.

5. Modification of Metallic Electrocatalysts by Plasma Treatment

Transition–metal compounds (TMCs), including metal oxides, metal phosphides, metal carbides, metal chalcogenides, and metal nitrides, have attracted research interests as these kinds

ADVANCED
SCIENCE NEWS
www.advancedsciencenews.com

Energy Technology
Generation, Conversion, Storage, Distribution

www.entechnol.de

Figure 8. A) LSV curves of pristine carbon a), B-doped carbon b), F-doped carbon c), and B- and F-dual-doped carbons d-e) by plasma treatment. B) Electron transfer number, and C) HO_2^{-} yields of the plasma-treated carbon products with B-doping and/or F-doping calculated from electrochemical measurements at the potential range from -1.0 to -0.3 V. Adapted with permission.[53] Copyright 2020, The Royal Society of Chemistry.

of materials are emerging as burgeoning families of cost-effective electrocatalysts.[31c] Most TMCs electrocatalysts with the tunable electronic interaction between metal ions and electronegative anions are likely to obtain desirable electronic distribution on metal active sites to benefit the electrocatalytic behaviors.[55] For example, metal oxides and metal phosphides have been recognized as promising electrocatalysts for the OER, with the foregoing considerations on the tunable M—OH bond energy, which should be essentially accounted for the variations of oxygen activity on different metallic sites.[56] In general, the catalytic activity of TMCs is governed by the transformation of valence states of the metallic active sites, sometimes also known as the surface reconstruction,[57] which can also be regulated by plasma treatment.

5.1. Transition Metal Oxides

Plasma technique was also used to increase the oxygen vacancy density of perovskite oxide $LaCoO_3$ with the procedures as illustrated in **Figure 9**A.[7a] The increased concentration of oxygen vacancy after the plasma treatment (sample termed as Sr-0.3-p) was confirmed by the oxygen temperature-programmed desorption (O_2-TPD) profile as shown in Figure 9B. The main desorption peak at $450 - 700\,°C$ corresponding to the chemical adsorption oxygen was assumed to be closely related to the oxygen vacancies in perovskite. Benefit from the massive oxygen vacancies incorporated in the perovskite oxide, much improved OER activity was observed with the Sr-0.3-p in liner sweep voltammetry (LSV) polarization curves (Figure 9C). Another example by introducing oxygen vacancies to cobalt oxide was reported by Ma et al.[58] Ar plasma treatment was inducted to regulate the oxidation state of Co ions in the oxide to promote the reversible

$Co–O \leftrightarrow Co–O–OH$ redox pathways within the active sites. As a result, improved redox electrochemical performance toward ORR/OER was achieved with the single-component oxide Co_3O_{4-x}. Air plasma treatment was applied to introduce oxygen vacancy to antimony-doped tin oxide (ATO) surface to benefit the electrocatalysis OER process with the corrosion resistant oxide support. The vacancy-rich ATO-supported NiFe layered double hydroxide exhibited improved performance toward OER in alkaline media.[59] As a results of the air plasma treatment, the binding energy of Ni^{2+} and Fe^{3+} shifted to more negative position, and low-valence Fe was formed, indicating the generation of oxygen vacancies. In addition, the formation of the defects led to a more hydrophilic surface to benefit the adsorption of reactants on the electrode.

To take advantage of the etching effect of plasma, plasma modification has been reported to treat the multilayer hollow $MnCo_2O_4$ spinel oxide. The plasma-engraving process (as illustrated in Figure 9D) gave rise to the surface roughness of the $MnCo_2O_4$ oxide surface, while preserved the multilayer hollow microsphere structure. Density functional theory calculation on density of states (DOS) demonstrated that the introduction of oxygen vacancies narrowed the bandgap by ≈0.15 eV, which increased the electronic conductivity of the bulk spinel oxide (Figure 9E). Meanwhile, the DOS projected on Co d orbital shifted to lower energies, indicating a weaker adsorption of the reaction intermediates to favor the OER process (Figure 9F).[60]

### 5.2. Other Metal Compounds

TMCs, like metal carbides, chalcogenides, and phosphides, have been explored as promising candidates for water splitting in acidic and alkaline conditions.[61] Simultaneously doping of N
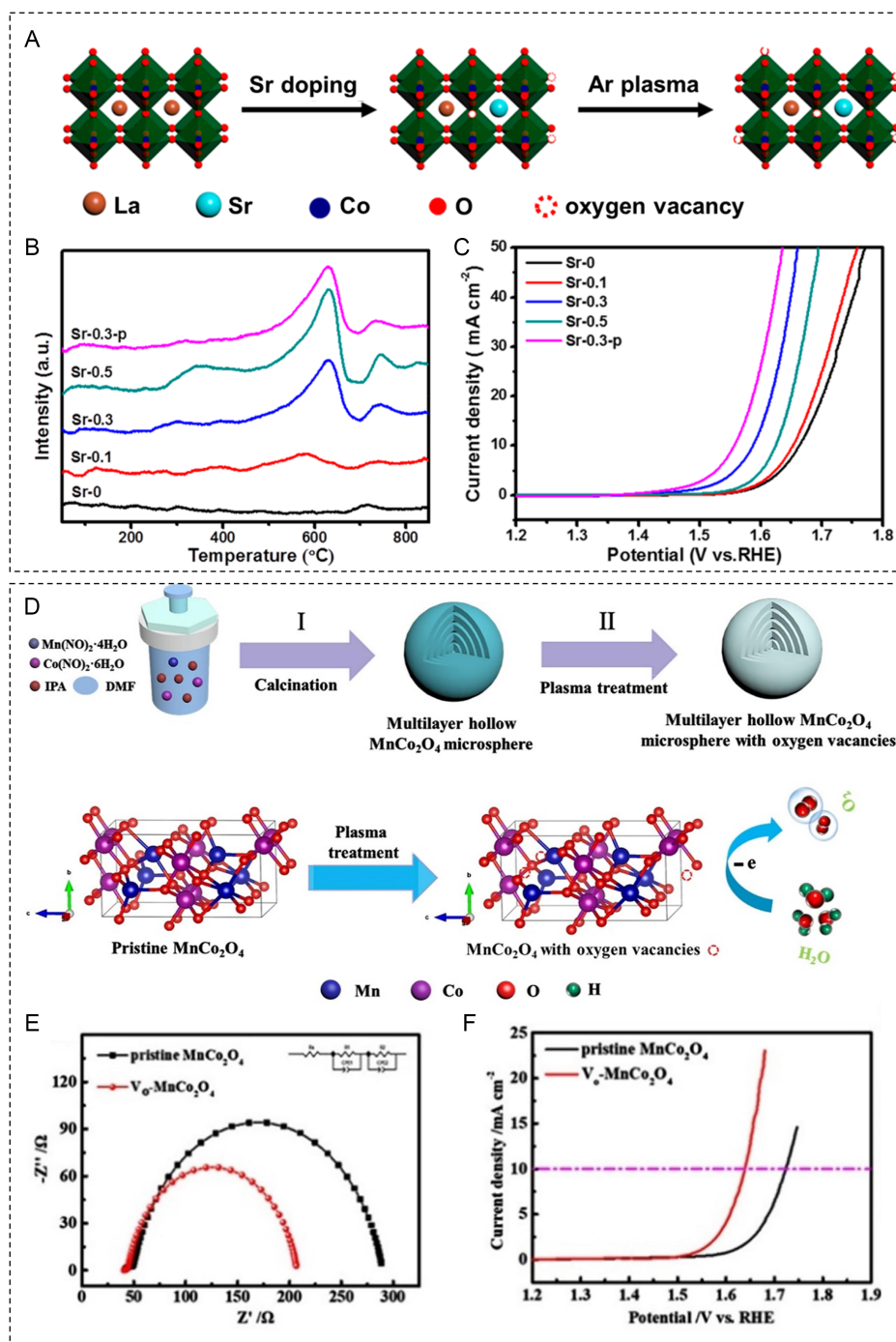
Figure 9. A) Schematic synthesis of oxygen vacancy rich $LaCoO_3$ perovskite by the combination strategy of Sr doping and Ar plasma treatment. B) O_2-TPD profiles of the $La_{1-x}Sr_xCoO_{3-\delta}$ perovskites after different Sr partial substitution and plasma treatment. C) LSV curves of the as-obtained $La_{1-x}Sr_xCoO_{3-\delta}$ perovskites. Adapted with permission.[7a] Copyright 2018, American Chemical Society. D) Scheme illustration of the preparation of oxygen vacancy-rich multilayer hollow $MnCo_2O_4$ microsphere by plasma treatment. E) The electrochemical impedance spectroscopy (EIS), and F) the OER polarization curves of oxygen vacancy-rich $MnCo_2O_4$ compared with pristine $MnCo_2O_4$ in 0.1 M KOH. Adapted with permission.[60] Copyright 2020, Elsevier B.V.

and P to NiCo alloy system was recently reported by Zhang et al. with highly reactive N_2/PH_3 plasma.[62] In their work, the NiCo alloy foam was applied as the substrate to form N-doped CoNi phosphide (N-CoNiP) by plasma modification, which exhibited much lower overpotentials of 78 mV for HER and 225 mV for OER at a current density of 10 mA cm^{-2} (**Figure 10**A,B). It was suggested that the exposure of active crystal planes (311) of the heterostructured Co_2NiP_4 phase contributed more
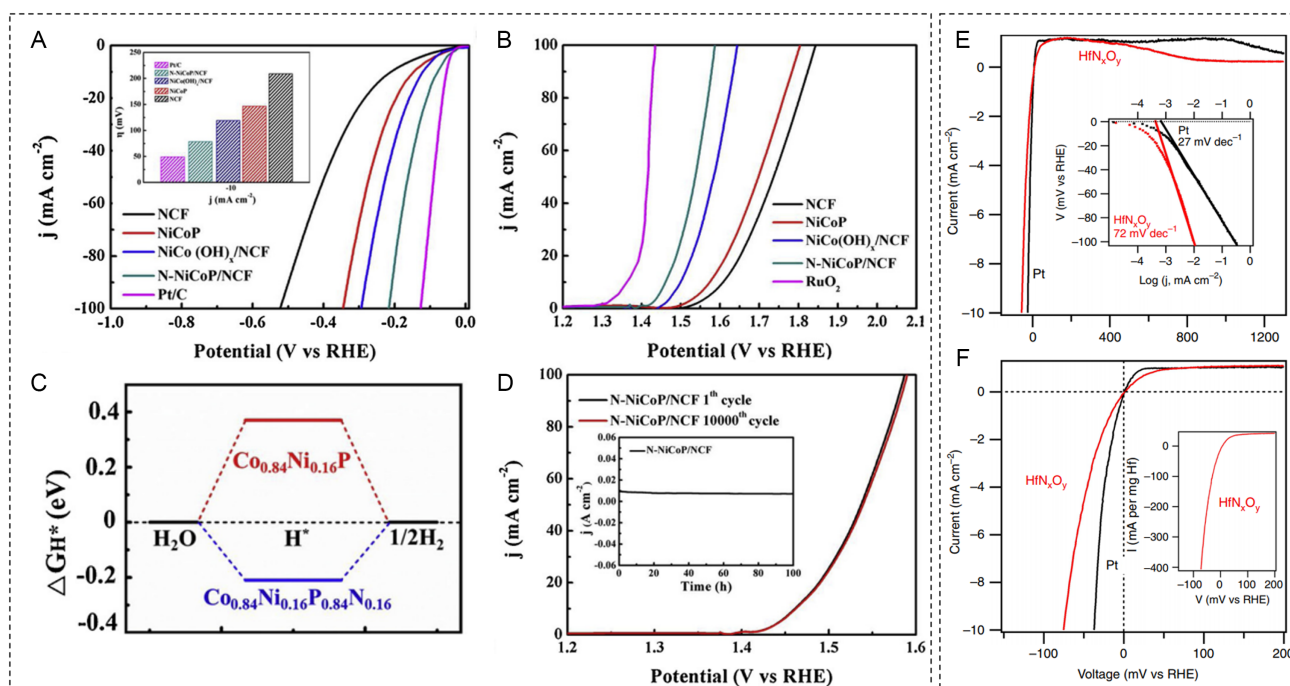
Figure 10. A) HER performance, and B) OER performance of the N-doped CoNi phosphide by plasma modification compared with the pristine counterparts and RuO_2 catalyst in 1 M KOH. C) The calculated HER free energy before and after N doping. D) Polarization curves of the N-doped CoNi phosphide before and after 10 000 cycles, with the inset plot of the long-term stability. Reproduced with permission.[62] Copyright 2019, Elsevier. E) Electrochemical HER and OER behaviors of the thin film HfN_xO_y electrode compared with Pt foil in acidic media with Tafel plot inset. F) Expanded view of the activity near-zero potential with calculated mass activity inset. Adapted with permission.[65] Copyright 2019, Elsevier B.V.

efficient active sites. The calculated free energy value (ΔG_H^*, as shown in Figure 10C) of N-doped CoNiP is −0.21 eV, which is much lower than the catalyst-H* state of CoNiP, indicating a lower energy barrier for absorbing H* in the HER process. As the microsized N-CoNiP was directly derived from the Ni foam substrate, the electrocatalytic performance of the active sites can be well maintained after 10 000 voltage cycles due to the strong coupling between the active sites and the substrates (Figure 10D).

Surface atom reorganization of metal phosphorus chalcogenides to increase the bifunctional catalytic activity has also been realized by plasma treatment. For example, Hao et al. reported the controlled O doping of $FePSe_3$ nanosheets. In this work, phase transformation by surface O doping accompanied with the origination of locally disordered lattice structures of the nanosheets was observed after Ar/O_2 plasma treatment.[6a] The as-obtained ultrathin $FePSe_3$-O exhibited metallic features, thus was able to possess fast charge transfer; meanwhile, the enhanced electrical state near the Fermi level was characterized, suggesting a stronger carrier density during electrocatalysis. Exceptional bifunctional activity toward ORR/OER with a narrow overpotential gap of 0.694 V was achieved. When used as the air electrode material in liquid zinc–air batteries, stable discharge–charge cycling was demonstrated to be maintained after 280 h. Similarly, O_2-plasma was used to realize controllably synthesis of hybrid metal compounds electrocatalysts, by directly constructing of 4–6 nm $NiFeO_x$ amorphous layer on the surface of NiFeP.[63] The synergistic effect between the NiFeP and

$NiFeO_x$ components brought higher charge transfer kinetics to the catalyst system; besides, the 3D hierarchical nanostructure with high surface area increased the contact with the electrolyte, thus resulting in extraordinary water oxidation performance in alkaline media. Another example was reported by Zheng et al. recently of using RF Ar plasma engraving to induce cobalt vacancy on Co_2N nanoarrays. The generated cobalt vacancy on the surface was tuned by adjusting the operating parameters (such as gas flow, power, and time) during Ar plasma treatment to manifest large pore area and proper surface N and Co vacancies for electrocatalysis.[64]

Transition metal oxynitrides (MN_xO_y, e.g., M = Ti, Ta, Hf) are stable in acids; if endowed with properly designed active sites, they could possibly be explored as promising alternatives to Pt for electrocatalysis in acidic environment. Processing Hf oxide with atmospheric N_2 plasma to form HfN_xO_y oxynitride was reported to be an effective way to increase the electrocatalytic activity toward HER and HOR in strong acids (Figure 10E,F).[65] It was proposed that the N incorporation played a critical role in enhancing the electrical conductivity of the Hf-based material.

Plasma is also conducted to create vacancies on the surface of transition metal compounds to benefit the electrocatalytic behaviors.[66] Ar plasma treatment was reported to apply to CoS nanoflowers to introduce abundant sulfur vacancies (CoS_{1-x}) on the catalyst surface.[67] The low coordinated Co atoms are likely to form more stable Co—N bond during the electrocatalysis nitrogen reduction reaction (NRR), while effectively suppress the HER catalysis due to the selective chemisorption of N_2 molecules.

**ADVANCED
SCIENCE NEWS**
www.advancedsciencenews.com

Energy Technology
Generation, Conversion, Storage, Distribution
www.entechnol.de

6. Plasma Treatment of Organometallic Electrocatalysts

Organometallic-based or derived electrocatalysts, such as metal phtalocyanines and porphyrins, are considered as promising candidates in electrocatalysis field.[68] These metallic macrocycle molecules usually need to be fixed on a carrier to maintain the stability of the active centers (metal–N_4) during the electrocatalytic reaction. The unique triangular trinuclear structure of metal–N_4 provides a high density of active sites and facilitates the reduction of dioxygen via a four-electron pathway,[69] thus has been applied in the ORR.

The morphology changes of the metallic macrocycles by heat-treatment process are unfavorable, as it could result in reduced available electrocatalytic active surface area. To surmount the drawback of pyrolysis procedure, Herrmann et al. first reported the plasma treatment of cobalt tetramethoxyphenylporphyrin (CoTMPP) to achieve uniform dispersion of CoN_4 centers onto the carbon matrix while avoiding the serious sintering effect accompanied with traditional heat treatment.[70] Harnisch et al. compared the electrocatalytic performance of the plasma-treated iron (II) phthalocyanine (FePc)-based carbon and the pyrolyzed counterpart.[71] It was found that though both pyrolysis and plasma treatment increased the surface concentration of nitrogen and oxygen with FePc carbon, the bulk composition of the catalyst could only be affected by pyrolysis.

Recently, Mohan et al. reported the N_2 plasma-assisted modification of the Fe–N–C catalyst (N-FeGly/C) derived from Fe precursors and glycine.[46b] Plasma modification was observed to significantly enhance the electrochemical capacitance by 8.5 times (**Figure 11**A), which was associated to the heteroatom functional groups on the carbon surface, and the obtained N-FeGly/C exhibited enhanced ORR electrocatalytic activity compared to that of the pristine FeGly/C (Figure 11B). On one hand, plasma exposure enabled the encapsulation of nitrogen coordinated iron sites, and improved the hydrophilicity of carbon matrix with heteroatoms incorporation. On the other, the increased surface roughness and porosity provided more accessible active sites. Electrochemical stability test results suggested insignificant changes both in the capacitive current and ORR polarization after 1000 potential cycles between 0 and 1.2 V in O_2-saturated electrolyte (Figure 11C,D), indicating the superior stability of the plasma-induced Fe–N–C active sites.

Etching effect of DBD plasma in water has also been utilized recently to modify the metal–organic framework (MOF)-based CoNi (CoNi-MOFs-DBD) electrocatalyst.[72] During the synthesis, water plasma was able to break the electrostatic interactions between the cationic primary metal layer and the interlayer to incorporate the catalyst with more heteroatom defects, meanwhile introduce a large number of hydroxyl groups to the surface, thereby improving the electrocatalytic properties for the overall water splitting.
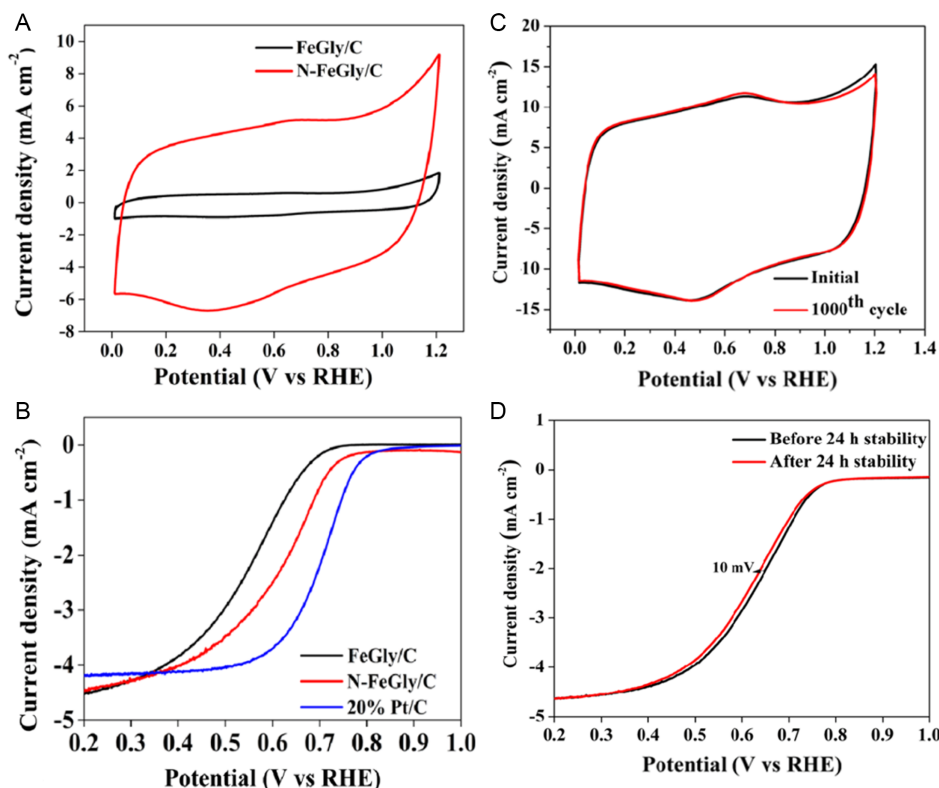
Figure 11. A) Cyclic voltammograms (CV) of FeGly/C and the as-prepared N-FeGly/C by plasma treatment as recorded in N_2-saturated 0.5 M H_2SO_4 solution. B) Liner sweep voltammograms (LSV) of FeGly/C and N-FeGly/C compared with commercial Pt/C in O_2-saturated 0.5 M H_2SO_4 electrolyte. C) CV curves and D) LSV curves of N-FeGly/C collected before and after 24 h durability test. Adapted with permission.[46b] Copyright 2021, American Chemical Society.

7. Conclusion and Perspectives

In conclusion, electrocatalysts modification to benefit the reaction behaviors at the surface has long been a highly concerned scientific issue. Plasma technique with the merits of easy operation, low pollution, and high efficiency has been used as a promising approach in modifying electrocatalysts for promoting better applications. This review comprehensively summarizes recent advances in applying plasma treatments for optimizing the chemical/physical properties of the electrocatalysts surface, including doping with functionalities, reorganizing surface atoms, introducing vacancies and/or defects, and partially reducing or oxidizing the active sites. The cutting-edge functional designs in regard to the mainstream electrocatalysts, including carbon materials, metal oxides, and other compounds, as well as organometals, have been highlighted. The mechanism behind nonthermal plasma processing and the effects of operating parameters are identified to provide insightful information for future research directions in ingenious electrocatalysts modification.

Despite gained noticeable popularity, plasma, as considered to be the "fourth state of matter," which involves complex physical collisions and ionization behaviors, remains to agnostic to be fully understood for proper applications.[73] Challenges still exist in the following perspectives: 1) Physical characterizations may be taken advantage of to diagnose the excited species in nonthermal plasma, for example, the active laser spectroscopy, including laser-two-photon-absorption laser-induced fluorescence (TALIF) and laser-induced fluorescence (LIF), which are commonly used to study the atmospheric pressure plasma, is recognized as good ways to obtain information on the chemical composition of the radicals.[74] Facilitated by these strategies, the complex reaction mechanism of plasma can be understood, only then can be used appropriately. 2) The energetic plasma-generated reactive species often bring surface etching/engraving effects while participating in the surface chemical bonding formation. The residues generated during plasma treatment may remain on the catalyst surface to cause unfavorable structural distortions.[3b,75] From this perspective, the controllability of operating parameters in plasma should be required to achieve precise functionalization of the electrocatalysts with desired composition and structure.[33,39,76] 3) Moreover, there are few theoretical research efforts toward the plasma treatment process for electrocatalysts modification. To define the interactions of plasma with materials surface, deeper investigation based on multidisciplinary theoretical calculations should be introduced. Nevertheless, challenges coexist with opportunities; plasma treatment is demonstrating a promising lead for developing effective electrocatalysts as a general, rapid, and environment-friendly way.

Conflict of Interest

The authors declare no conflict of interest.

[1] C. Liu, G. P. Vissokov, B. W. L. Jang, *Catal. Today* **2002**, *72*, 173.

[2] F. Yu, M. Liu, C. Ma, L. Di, B. Dai, L. Zhang, *Nanomaterials* **2019**, *9*, 1436.

[3] a) C. Liu, J. Zou, K. Yu, D. Cheng, Y. Han, J. Zhan, C. Ratanatawanate, B. W. L. Jang, *Pure Appl. Chem.* **2006**, *78*, 1227; b) Z. Wang, Y. Zhang, E. C. Neyts, X. Cao, X. Zhang, B. W. L. Jang, C. Liu, *ACS Catal.* **2018**, *8*, 2093.

[4] Y. Zhang, R. S. Rawat, H. J. Fan, *Small Methods* **2017**, *1*, 1700164.

[5] V. I. Pârvulescu, M. Magureanu, P. Lukes, in *Plasma Chemistry and Catalysis in Gases and Liquids*, Wiley-VCH Verlag GmbH & Co. KGaA, Hoboken, NJ **2012**.

[6] a) Y. Hao, A. Huang, S. Han, H. Huang, J. Song, X. Sun, Z. Wang, L. Li, F. Hu, J. Xue, S. Peng, *ACS Appl. Mater. Interfaces* **2020**, *12*, 29393; b) K. Xu, H. Cheng, H. Lv, J. Wang, L. Liu, S. Liu, X. Wu, W. Chu, C. Wu, Y. Xie, *Adv. Mater.* **2018**, *30*, 1703322; c) X. Wang, L. Zhuang, Y. Jia, H. Liu, X. Yan, L. Zhang, D. Yang, Z. Zhu, X. Yao, *Angew. Chem., Int. Ed.* **2018**, *57*, 16421.

[7] a) Y. Lu, A. Ma, Y. Yu, R. Tan, C. Liu, P. Zhang, D. Liu, J. Gui, *ACS Sustain. Chem. Eng.* **2019**, *7*, 2906; b) Y. Tian, Y. Ye, X. Wang, S. Peng, Z. Wei, X. Zhang, W. Liu, *Appl. Catal. A: General* **2017**, *529*, 127; c) L. Tao, Q. Wang, S. Dou, Z. Ma, J. Huo, S. Wang, L. Dai, *Chem. Commun.* **2016**, *52*, 2764; d) Y. Tian, R. Mei, D.-Z. Xue, X. Zhang, W. Peng, *Electrochim. Acta* **2016**, *219*, 781.

[8] a) W. Zhong, J. Chen, P. Zhang, L. Deng, L. Yao, X. Ren, Y. Li, H. Mi, L. Sun, *J. Mater. Chem. A* **2017**, *5*, 16605; b) L. Li, H. Yang, J. Miao, L. Zhang, H.-Y. Wang, Z. Zeng, W. Huang, X. Dong, B. Liu, *ACS Energy Lett.* **2017**, *2*, 294.

[9] H. Mistry, A. S. Varela, C. S. Bonifacio, I. Zegkinoglou, I. Sinev, Y.-W. Choi, K. Kisslinger, E. A. Stach, J. C. Yang, P. Strasser, B. R. Cuenya, *Nat. Commun.* **2016**, *7*, 12123.

[10] a) J. Zhou, H. Yue, F. Qi, H. Wang, Y. Chen, *Int. J. Hydrogen Energy* **2017**, *42*, 27004; b) I. Kondratowicz, M. Nadolska, S. Şahin, M. Łapiński, M. Prześniak-Welenc, M. Sawczak, E. H. Yu, W. Sadowski, K. Żelechowska, *Appl. Surf. Sci.* **2018**, *440*, 651.

[11] a) A. Kuznetsova, I. Popova, J. T. Yates, M. J. Bronikowski, C. B. Huffman, J. Liu, R. E. Smalley, H. H. Hwu, J. G. Chen, *J. Am. Chem. Soc.* **2001**, *123*, 10699; b) T. A. Saleh, *Appl. Surf. Sci.* **2011**, *257*, 7746; c) J. M. Simmons, B. M. Nichols, S. E. Baker, M. S. Marcus, O. M. Castellini, C. S. Lee, R. J. Hamers, M. A. Eriksson, *J. Phys. Chem. B* **2006**, *110*, 7113; d) D. B. Mawhinney, V. Naumenko, A. Kuznetsova, J. T. Yates, J. Liu, R. E. Smalley, *J. Am. Chem. Soc.* **2000**, *122*, 2383; e) P. M. Ajayan, T. W. Ebbesen, T. Ichihashi, S. Iijima, K. Tanigaki, H. Hiura, *Nature* **1993**, *362*, 522.

[12] H. Liang, F. Ming, H. N. Alshareef, *Adv. Mater.* **2018**, *8*, 1801804.

[13] M. Laroussi, *Plasma Process. Polym.* **2005**, *2*, 391.

[14] a) M. J. Pavlovich, D. S. Clark, D. B. Graves, *Plasma Sources Sci. Technol.* **2014**, *23*, 065036; b) M. C. Kim, S. H. Yang, J. H. Boo, J. G. Han, *Surf. Coat. Technol.* **2003**, *174–175*, 839.

[15] V. V. Kovačević, B. P. Dojčinović, M. Jović, G. M. Roglić, B. M. Obradović, M. M. Kuraica, *J. Phys. D: Appl. Phys.* **2017**, *50*, 155205.

[16] T. Hammer, T. Kappes, M. Baldauf, *Catal. Today* **2004**, *89*, 5.

[17] B. Ouyang, Y. Zhang, X. Xia, R. S. Rawat, H. J. Fan, *Mater. Today Nano* **2018**, *3*, 28.

[18] H. Yu, G. Liu, M. Wang, R. Ren, G. Shim, J. Y. Kim, M. X. Tran, D. Byun, J. K. Lee, *ACS Appl. Mater. Interfaces* **2020**, *12*, 5820.

[19] a) T. Zhang, J. Wu, J. Chen, Q. Pan, X. Wang, H. Zhong, R. Tao, J. Yan, Y. Hu, X. Ye, C. Chen, J. Chen, *ACS Appl. Mater. Interfaces* **2021**, *13*, 24682; b) S. Major, S. Kumar, M. Bhatnagar, K. Chopra, *Appl. Phys. Lett.* **1986**, *49*, 394.

[20] Y.-P. Lin, Y. Ksari, J. Prakash, L. Giovanelli, J.-C. Valmalette, J.-M. Themlin, *Carbon* **2014**, *73*, 216.

[21] a) M. Weyers, M. Sato, *Appl. Phys. Lett.* **1993**, *62*, 1396; b) P. R. McCurdy, C. I. Butoi, K. L. Williams, E. R. Fisher, *J. Phys. Chem. B* **1999**, *103*, 6919; c) G. Singh, D. S. Sutar, V. Divakar Botcha, P. K. Narayanam, S. S. Talwar, R. S. Srinivasa, S. S. Major, *Nanotechnology* **2013**, *24*, 355704.

[22] a) P. Kumar, M. Singh, R. K. Sharma, G. B. Reddy, *J. Alloys Compd.* **2016**, *671*, 440; b) H. Liang, A. N. Gandi, D. H. Anjum, X. Wang, U. Schwingenschlögl, H. N. Alshareef, *Nano Lett.* **2016**, *16*, 7718; c) H. Liang, C. Xia, Q. Jiang, A. N. Gandi, U. Schwingenschlögl, H. N. Alshareef, *Nano Energy* **2017**, *35*, 331; d) L. Ma, S. Hu, P. Li, Q. Wang, H. Ma, W. Li, *J. Phys. Chem. Solids* **2018**, *118*, 166; e) C. H. A. Wong, Z. Sofer, K. Klímová, M. Pumera, *ACS Appl. Mater. Interfaces* **2016**, *8*, 31849.

[23] A. Shen, Y. Zou, Q. Wang, R. A. Dryfe, X. Huang, S. Dou, L. Dai, S. Wang, *Angew. Chem.* **2014**, *126*, 10980.

[24] Z. Liu, Z. Zhao, Y. Wang, S. Dou, D. Yan, D. Liu, Z. Xia, S. Wang, *Adv. Mater.* **2017**, *29*, 1606207.

[25] J. Zhang, Z. Zhao, Z. Xia, L. Dai, *Nat. Nanotechnol.* **2015**, *10*, 444.

[26] W. Gu, L. Hu, X. Zhu, C. Shang, J. Li, E. Wang, *Chem. Commun.* **2018**, *54*, 12698.

[27] D. A. Kuznetsov, B. Han, Y. Yu, R. R. Rao, J. Hwang, Y. Román-Leshkov, Y. Shao-Horn, *Joule* **2018**, *2*, 225.

[28] a) Y.-J. Zhang, A. A. Peterson, *Phys. Chem. Chem. Phys.* **2015**, *17*, 4505; b) X. Nie, G. L. Griffin, M. J. Janik, A. Asthagiri, *Catal. Commun.* **2014**, *52*, 88.

[29] D. Gao, I. Zegkinoglou, N. J. Divins, F. Scholten, I. Sinev, P. Grosse, B. Roldan Cuenya, *ACS Nano* **2017**, *11*, 4825.

[30] Y. Zhang, B. Ouyang, K. Xu, X. Xia, Z. Zhang, R. S. Rawat, H. J. Fan, *Small* **2018**, *14*, 1800340.

[31] a) Y. Gao, Z. Zhao, H. Jia, X. Yang, X. Lei, X. Kong, F. Zhang, *J. Mater. Sci.* **2019**, *54*, 14515; b) Y. Xue, S. Sun, Q. Wang, Z. Dong, Z. Liu, *J. Mater. Chem. A* **2018**, *6*, 10595; c) A. Zhang, Y. Liang, H. Zhang, Z. Geng, J. Zeng, *Chem. Soc. Rev.* **2021**, *50*, 9817.

[32] M. Gołda, M. Brzychczy-Włoch, M. Faryna, K. Engvall, A. Kotarba, *Mater. Sci. Eng.: C* **2013**, *33*, 4221.

[33] X. Sun, J. Bao, K. Li, M. D. Argyle, G. Tan, H. Adidharma, K. Zhang, M. Fan, P. Ning, *Adv. Funct. Mater.* **2021**, *31*, 2006287.

[34] D. Lu, D. Wu, J. Jin, L. Chen, *Electrochim. Acta* **2016**, *215*, 66.

[35] J. M. Carlsson, M. Scheffler, *Phys. Rev. Lett.* **2006**, *96*, 046806.

[36] Q. Chen, B. Song, X. Li, R. Wang, S. Wang, S. Xu, F. Reniers, C. H. Lam, *Ind. Eng. Chem. Res.* **2021**, *60*, 16813.

[37] H. R. Khaledian, P. Zolfaghari, V. Elhami, M. Aghbolaghy, S. Khorram, A. Karimi, A. Khataee, *Molecules* **2019**, *24*, 383.

[38] C. Chen, A. Ogino, X. Wang, M. Nagatsu, *Diamond Relat. Mater.* **2011**, *20*, 153.

[39] J. Duch, M. Mazur, M. Golda-Cepa, J. Podobiński, W. Piskorz, A. Kotarba, *Carbon* **2018**, *137*, 425.

[40] W. He, Y. Wang, C. Jiang, L. Lu, *Chem. Soc. Rev.* **2016**, *45*, 2396.

[41] a) J. Quílez-Bermejo, E. Morallón, D. Cazorla-Amorós, *Carbon* **2020**, *165*, 434; b) K. Gong, F. Du, Z. Xia, M. Durstock, L. Dai, *Science* **2009**, *323*, 760.

[42] L. Yang, S. Jiang, Y. Zhao, L. Zhu, S. Chen, X. Wang, Q. Wu, J. Ma, Y. Ma, Z. Hu, *Angew. Chem., Int. Ed.* **2011**, *50*, 7132.

[43] S. K. Singh, K. Takeyasu, J. Nakamura, *Adv. Mater.* **2019**, *31*, 1804297.

[44] P. Subramanian, A. Cohen, E. Teblum, G. D. Nessim, E. Bormasheko, A. Schechter, *Electrochem. Commun.* **2014**, *49*, 42.

[45] M. K. Hoque, J. A. Behan, J. Creel, J. G. Lunney, T. S. Perova, P. E. Colavita, *Front. Chem.* **2020**, *8*, 593932.

[46] a) R. Mohan, A. Modak, A. Schechter, *Catal. Sci. Technol.* **2020**, *10*, 1675; b) R. Mohan, A. Modak, A. Schechter, *ACS Appl. Energy Mater.* **2021**, *4*, 564; c) O. Kazak, Y. R. Eker, H. Bingol, A. Tor, *Chem. Eng. J.* **2017**, *325*, 564.

[47] R. Mohan, A. Modak, A. Schechter, *ACS Sustain. Chem. Eng.* **2019**, *7*, 11396.

[48] K. Waki, R. A. Wong, H. S. Oktaviano, T. Fujio, T. Nagai, K. Kimoto, K. Yamada, *Energy Environ. Sci.* **2014**, *7*, 1950.

[49] H. Zhang, K. Lv, B. Fang, M. C. Forster, R. Dervişoğlu, L. B. Andreas, K. Zhang, S. Chen, *Electrochim. Acta* **2018**, *292*, 942.

[50] Y. Habibi, *Chem. Soc. Rev.* **2014**, *43*, 1519.

[51] S. V. Sawant, A. W. Patwardhan, J. B. Joshi, K. J. C. E. J. Dasgupta, *Chem. Eng. J.* **2022**, *427*, 131616.

[52] a) X. Sun, Y. Zhang, P. Song, J. Pan, L. Zhuang, W. Xu, W. Xing, *ACS Catal.* **2013**, *3*, 1726; b) Y. Lv, L. Yang, D. Cao, *ACS Appl. Mater. Interfaces* **2017**, *9*, 32859.

[53] C. Chokradjaroen, S. Kato, K. Fujiwara, H. Watanabe, T. Ishii, T. Ishizaki, *Sustain. Energy Fuels* **2020**, *4*, 4570.

[54] O. L. Li, Z. Shi, H. Lee, T. Ishizaki, *Sci. Rep.* **2019**, *9*, 12704.

[55] a) T. Sakthivel, X. Huang, Y. Wu, S. Rtimi, *Chem. Eng. J.* **2020**, *379*, 122297; b) J. Yu, Y. Dai, Q. He, D. Zhao, Z. Shao, M. Ni, *Mater. Rep.: Energy* **2021**, *1*, 100024.

[56] a) A. Dutta, N. Pradhan, *J. Phys. Chem. Lett.* **2017**, *8*, 144; b) H.-F. Wang, C. Tang, B.-Q. Li, Q. Zhang, *Inorg. Chem. Front.* **2018**, *5*, 521.

[57] a) Y. Zhu, Q. Lin, Y. Zhong, H. A. Tahini, Z. Shao, H. Wang, *Energy Environ. Sci.* **2020**, *13*, 3361; b) J. Chen, H. Chen, T. Yu, R. Li, Y. Wang, Z. Shao, S. Song, *Electrochem. Energy Rev.* **2021**, *4*, 566.

[58] L. Ma, S. Chen, Z. Pei, H. Li, Z. Wang, Z. Liu, Z. Tang, J. A. Zapien, C. Zhi, *ACS Nano* **2018**, *12*, 8597.

[59] C. Lei, W. Li, G. Wang, L. Zhuang, J. Lu, L. Xiao, *Chem. Res. Chin. Univ.* **2021**, *37*, 293.

[60] K. Zeng, W. Li, Y. Zhou, Z. Sun, C. Lu, J. Yan, J.-H. Choi, R. Yang, *Chem. Eng. J.* **2021**, *421*, 127831.

[61] X. Peng, C. Pi, X. Zhang, S. Li, K. Huo, P. K. Chu, *Sustain. Energy Fuels* **2019**, *3*, 366.

[62] R. Zhang, J. Huang, G. Chen, W. Chen, C. Song, C. Li, K. Ostrikov, *Appl. Catal., B* **2019**, *254*, 414.

[63] C. Zhang, N. Gong, C. Ding, Y. Li, W. Peng, G. Zhang, F. Zhang, X. Fan, *Int. J. Hydrogen Energy* **2019**, *44*, 26118.

[64] J. Zheng, A. Xu, A. Wu, X. Li, *ACS Appl. Mater. Interfaces* **2021**, *13*, 21231.

[65] X. Yang, F. Zhao, Y.-W. Yeh, R. S. Selinsky, Z. Chen, N. Yao, C. G. Tully, Y. Ju, B. E. Koel, *Nat. Commun.* **2019**, *10*, 1543.

[66] X. Wang, R. Zhou, C. Zhang, S. Xi, M. W. M. Jones, T. Tesfamichael, A. Du, K. Gui, K. Ostrikov, H. Wang, *J. Mater. Chem. A* **2020**, *8*, 9278.

[67] C. Li, R. Xu, S. Ma, Y. Xie, K. Qu, H. Bao, W. Cai, Z. Yang, *Chem. Eng. J.* **2021**, *415*, 129018.

[68] a) A. Morozan, S. Campidelli, A. Filoramo, B. Jousselme, S. Palacin, *Carbon* **2011**, *49*, 4839; b) J. H. Zagal, S. Griveau,

K. I. Ozoemena, T. Nyokong, F. Bedioui, *J. Nanosci. Nanotechnol.* **2009**, *9*, 2201.

[69] R. Liu, C. von Malotki, L. Arnold, N. Koshino, H. Higashimura, M. Baumgarten, K. Müllen, *J. Am. Chem. Soc.* **2011**, *133*, 10372.

[70] I. Herrmann, V. Brüser, S. Fiechter, H. Kersten, P. Bogdanoff, *J. Electrochem. Soc.* **2005**, *152*, A2179.

[71] F. Harnisch, N. A. Savastenko, F. Zhao, H. Steffen, V. Brüser, U. Schröder, *J. Power Sources* **2009**, *193*, 86.

[72] W. Zhang, B. Zhang, Y. Li, E. Zhang, Y. Zhang, Q. Wang, Y. Cong, *Int. J. Hydrogen Energy* **2022**, *47*, 1633.

[73] a) F. F. Chen, in *Introduction to Plasma Physics and Controlled Fusion*, Springer International Publishing, Switzerland **2016**; b) J. A. Bittencourt, in *Fundamentals of Plasma Physics*, Springer-Verlag New York, Inc., Cham, Switzerland **2004**; c) O. Baranov, K. Bazaka, H. Kersten, M. Keidar, U. Cvelbar, S. Xu, I. Levchenko, *Appl. Phys. Rev.* **2017**, *4*, 041302.

[74] a) Y. Yue, X. Pei, D. Gidon, F. Wu, S. Wu, X. Lu, *Plasma Sources Sci. Technol.* **2018**, *27*, 064001; b) M. Keidar, D. Yan, J. H. Sherman, in *Cold Plasma Cancer Therapy*, Morgan & Claypool Publishers, San Rafael, CA, United States **2019**, pp. 2-1–2-7; c) I. V. Adamovich, W. R. Lempert, *Plasma Phys. Controlled Fusion* **2014**, *57*, 014001.

[75] K. Dong, J. Liang, Y. Wang, Y. Ren, Z. Xu, H. Zhou, L. Li, Q. Liu, Y. Luo, T. Li, A. M. Asiri, Q. Li, D. Ma, X. Sun, *Chem. Catal.* **2021**, *1*, 1437.

[76] J. Ortiz-Medina, Z. Wang, R. Cruz-Silva, A. Morelos-Gomez, F. Wang, X. Yao, M. Terrones, M. Endo, *Adv. Mater.* **2019**, *31*, 1805717.

Jiayi Tang obtained her M.S. degree in materials engineering from the Institute of Process Engineering, Chinese Academy of Sciences (CAS) in 2018. She is currently a Ph.D. student in Curtin University under the supervision of Prof. Zongping Shao. Her research interests are dedicated to the rational design of electrode materials and electrode structures for clean energy conversion devices, e.g., fuel cells and membrane electrolyzer cells.

Chao Su received her Ph.D. degree in chemical engineering at Nanjing Tech University, China, in 2012. She is a recipient of Australian Research Council (ARC) Discovery Early Career Researcher Award (DECRA) Fellow. Currently, she is a professor at the School of Energy and Power, Jiangsu University of Science and Technology, China. Her research focuses on the development of functional materials for electrochemical energy conversion and storage technologies, such as fuel cells, metal–air batteries, and water splitting.

Zongping Shao is a John Curtin Distinguished Professor at Curtin University, Australia, and also a professor at Nanjing Tech University, China. He obtained his Ph.D. degree from Dalian Institute of Chemical Physics, China, in 2000. He worked as a visiting scholar at Institut de Researches Sur La Catalyse, CNRS, France, and then a postdoctoral fellow at California Institute of Technology, USA, from 2000 to 2005. His current research interests include fuel cells, lithium-ion batteries, metal–air batteries, solar cells, and oxygen-permeable membranes. He has been recognized as a Highly-Cited Researcher by Clarivate Analytics since 2017.